Multilevel Computations of Dispersed Drug Release

Wei Zhao, Dmitry E. Pelinovsky
Department of Mathematics, McMaster University, Hamilton, Ontario, Canada, L8S 4K1

Received 1 March 2012; accepted 5 November 2012
Published online 26 December 2012 in Wiley Online Library (wileyonlinelibrary.com).
DOI 10.1002/num.21761

We study a mathematical model of drug release from controlled delivery systems with initial drug loading higher than solubility. The model combines dissolution, diffusion, swelling, and erosion mechanisms of drug delivery. Multilevel methods are introduced to solve the governing system of diffusion equations numerically with better accuracy and lower computational costs compared with the finite element methods. Numerical examples are given to demonstrate the advantages of the multilevel methods. Numerical solutions are compared to exact and approximate solutions of the reduced models. © 2012 Wiley Periodicals, Inc. Numer Methods Partial Differential Eq 29: 1391–1415, 2013

Keywords: controlled drug release; mathematical modeling; system of diffusion equations; multilevel scheme

I. INTRODUCTION

To improve the performance of drug delivery systems, controlled release systems (CRS) were proposed to replace the traditional delivery systems (TDS). Compared to TDS, the key advantages of CRS are the reduction of the dosing frequency and the elimination of the possible overdosing. The purpose of CRS is to maintain the drug concentration in body tissues at a desired value as long as possible. To achieve this, the drug release rate is needed to be controlled at the level of the drug consuming rate. This requires us to simulate the release kinetics from a system of diffusion equations.

Matrix and membrane systems are popularly used in CRS. The term "matrix" indicates a three-dimensional network. In this article, we investigate the matrix systems obtained by embedding of a drug into a polymer. Several mathematical models have been proposed to predict drug release kinetics from matrix CRS [1–3]. The model we consider deals with hydrophilic and degradable polymeric matrices and dispersed drug release, where dispersed drug release stands for the drug release in the case that the initial drug loading C_0 is higher than the drug solubility $C_{\mathrm{d,s}}$. For convenience, C_0 and $C_{\mathrm{d,s}}$ are defined as volume percentage instead of mass percentage. Furthermore,

Correspondence to: Dmitry E. Pelinovsky, Department of Mathematics, McMaster University, Hamilton, Ontario, Canada, L8S 4K1 (e-mail: dmpeli@math.mcmaster.ca)
Contract grant sponsor: Mathematics of Information Technology and Complex Systems (MITACS); MITACS Elevate Postdoctoral fellowship

dispersed drug release is typically described under the assumption that dissolution is much faster than diffusion [4, 5]. In practice, however, many drugs only possess low to medium solubility. Their release should be controlled by both diffusion and dissolution. Hence, our model combines not only polymer swelling and erosion but also drug diffusion and dissolution mechanisms.

Various efforts have been made to obtain the analytical solutions of the governing equations describing dispersed drug release. Higuchi [6, 7] proposed the pseudo steady-state approximation (PSSA), when a linear distribution is used for the drug concentration, for slabs and spheres with $C_0 > C_{d,s}$ and $C_0 \gg C_{d,s}$, in a perfect sink. An exact solution was developed by Paul and McSpandden [1] for the planar geometry beyond the PSSA. Lee [4] used an integral method to obtain more accurate approximate analytical solutions compared with those in PSSA. Using the PSSA, Zhou and Wu [3, 8] derived analytic solutions for slabs, spheres, and sphere ensembles with $C_0 > C_{d,s}$ and $C_0 \gg C_{d,s}$ in a finite medium with boundary layer effects. Analytical solutions for two-dimensional matrix tablets in a perfect sink were also constructed in Ref. [9].

Exact and approximate analytical solutions are only valid for the release process up to a time instance when all the dispersed drug is dissolved. Hence, numerical methods are needed to approximate a solution for the entire release process. Finite element and finite difference methods are usually applied in numerical simulations of the matrix CRS [2, 5, 10]. To obtain a better approximation with lower computational costs, we introduce here a multilevel method to solve the system of diffusion equations numerically. The multilevel methods have been successfully applied to elliptic equations in the literature [11–14]. Compared with the classical finite element method, the multilevel scheme achieves the same accuracy much faster. We will provide several numerical examples to demonstrate advantages of the multilevel methods in the context of modeling of the matrix CRS.

This article is organized as follows. In Section II, we introduce the model describing dispersed drug release from swellable and erodible matrix systems. In Section III, we analyze the multilevel method for solving the governing system of diffusion equations numerically. The resulting linear system of equations associated with the multilevel scheme is proved to be well-conditioned. In Section IV, numerical examples are provided to demonstrate the advantages of the multilevel scheme. We also compare our simulations with exact and approximate solutions of the reduced models. The summary of our work is given in Section V. Appendices A, B, and C give details of the derivation of exact and approximate solutions of reduced models, which are used for comparison with numerical computations.

II. MATHEMATICAL MODEL

We first set up a model describing dispersed drug release from swellable and erodible matrix system. Then, we use a scaling transformation to construct a dimensionless model that is suitable for numerical solutions.

A. Formulation

Let's consider a polymer matrix system with initial drug loading C_0 higher than the drug solubility $C_{d,s}$. As dissolved drug diffuses out, undissolved (dispersed) drug dissolves. Fick's second law of diffusion and linear dissolution are assumed. Other non-Fickian types of diffusion are also possible and have been considered in the past [15–17].

The evolution of water penetration, drug diffusion, and dissolution is described by the following three parabolic equations on the domain $\Omega \subset \mathbb{R}^3$ and time $t > 0$,

$$\frac{\partial C_{\mathrm{w}}}{\partial t} = \nabla \cdot (D_{\mathrm{w}} \nabla C_{\mathrm{w}}), \tag{1}$$

$$\frac{\partial C_{\mathrm{d}}}{\partial t} = \nabla \cdot (D_{\mathrm{d}} \nabla C_{\mathrm{d}}) + k_{\mathrm{d}}(C_{\mathrm{d,s}} - C_{\mathrm{d}})H(C_{\mathrm{u}}), \tag{2}$$

$$\frac{\partial C_{\mathrm{u}}}{\partial t} = -k_{\mathrm{d}}(C_{\mathrm{d,s}} - C_{\mathrm{d}})H(C_{\mathrm{u}}), \tag{3}$$

where C_{w}, C_{d}, and C_{u} denote the concentration of water, dissolved, and undissolved (dispersed) drug as volume percentage, D_{w} and D_{d} represent the water penetration and the drug diffusion coefficients, and k_{d} denotes the dissolution rate constant. Note that H is the Heaviside step function defined by

$$H(x) = \begin{cases} 0, & x \le 0, \\ 1, & x > 0. \end{cases}$$

The step function in (2)–(3) is presented because dissolution takes place where the concentration C_{u} of undissolved (dispersed) drug is greater than 0.

In this article, we study the drug release from a spherical matrix with initial radius R_0. Water penetration causes the polymer swelling which is supposed to be homogeneous in the radial direction. Polymer erosion is assumed on the surface of the matrix. Hence, the positions $R(t)$ of the polymer swelling front and erosion front are identical and $R_0 = R(0)$. Therefore, the domain $\Omega \subset \mathbb{R}^3$ for system (1)–(3) is a ball of radius $R(t)$, with boundary conditions at the sphere of radius $R(t)$. In the spherical coordinates under the spherical symmetry, Eqs. (1)–(3) are rewritten as follows,

$$\frac{\partial C_{\mathrm{w}}}{\partial t} = \frac{1}{r^2}\frac{\partial}{\partial r}\left(r^2 D_{\mathrm{w}} \frac{\partial C_{\mathrm{w}}}{\partial r}\right), \tag{4}$$

$$\frac{\partial C_{\mathrm{d}}}{\partial t} = \frac{1}{r^2}\frac{\partial}{\partial r}\left(r^2 D_{\mathrm{d}} \frac{\partial C_{\mathrm{d}}}{\partial r}\right) + k_{\mathrm{d}}(C_{\mathrm{d,s}} - C_{\mathrm{d}})H(C_{\mathrm{u}}), \tag{5}$$

$$\frac{\partial C_{\mathrm{u}}}{\partial t} = -k_{\mathrm{d}}(C_{\mathrm{d,s}} - C_{\mathrm{d}})H(C_{\mathrm{u}}), \tag{6}$$

where $0 < r < R(t)$ and $t > 0$.

Initially, the drug loading C_0 is greater than the solubility $C_{\mathrm{d,s}}$, and no water exists in the matrix. Thus, we have

$$t = 0, \quad 0 \le r \le R_0 : \quad C_{\mathrm{w}} = 0, \quad C_{\mathrm{d}} = C_{\mathrm{d,s}}, \quad C_{\mathrm{u}} = C_0 - C_{\mathrm{d,s}} > 0. \tag{7}$$

At the swelling front $r = R(t)$, equilibrium water concentration $C_{\mathrm{w,e}}$ as volume percentage in fully swollen polymeric matrix is assumed, whereas a perfect sink condition for the dissolved drug is considered. Symmetry conditions are applied at the center of the matrix. Hence, the boundary conditions are

$$t > 0, \quad r = R(t) : \quad C_{\mathrm{w}} = C_{\mathrm{w,e}}, \quad C_{\mathrm{d}} = 0; \tag{8}$$

$$t > 0, \quad r = 0 : \quad \frac{\partial C_{\mathrm{w}}}{\partial r} = 0, \quad \frac{\partial C_{\mathrm{d}}}{\partial r} = 0. \tag{9}$$

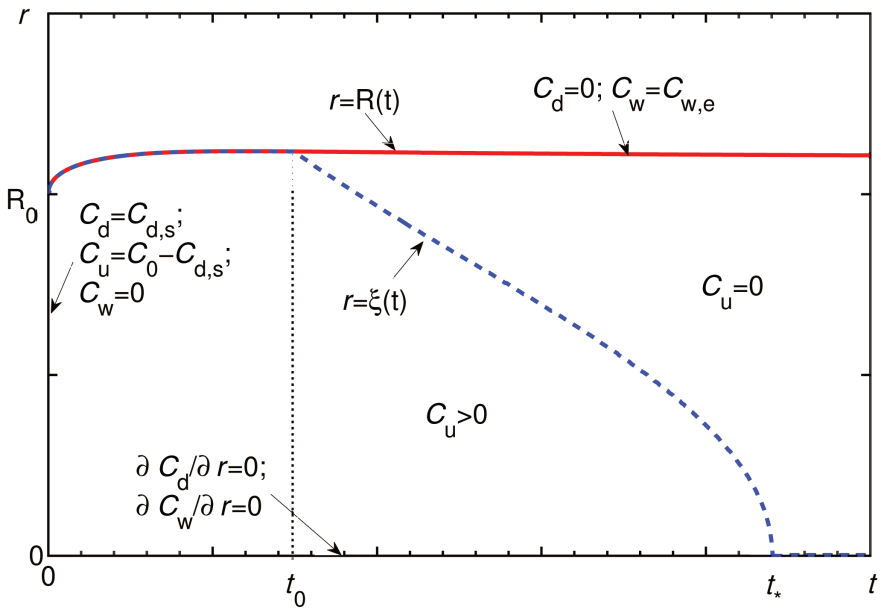

FIG. 1. Dynamics of the drug delivery system. [Color figure can be viewed in the online issue, which is available at wileyonlinelibrary.com.]

The rate of polymer erosion is taken in the form,

$$\frac{1}{A_s}\frac{dV_p}{dt} = -k_p,$$

where V_p stands for the volume of the polymer, k_p denotes the polymer erosion constant, and A_s represents the surface area of the matrix, which is $4\pi R(t)^2$ at time t in our case. At any time, the total volume of the matrix is sum of the volumes of water, dissolved and dispersed drug. Therefore, we have

$$\frac{4}{3}\pi R(t)^3 = \int_0^{R(t)} 4\pi r^2 C_w(r,t)dr + \int_0^{R(t)} 4\pi r^2 [C_d(r,t) + C_u(r,t)]dr + \left(V_{p,0} - \int_0^t k_p[4\pi R(t)^2]dt\right), \tag{10}$$

where $V_{p,0}$ stands for the initial volume of the polymer.

Figure 1 shows the dynamics of the drug delivery system. At time $t = 0$, the boundary (outer boundary) of the matrix is at $r = R_0$. As time evolves, the outer boundary $R(t)$ moves because of water penetration and polymer erosion. The boundary (inner boundary) of the dispersed drug is denoted by $\xi(t)$, which is defined as the smallest value of r where $C_u = 0$, and the Heaviside step function H in (5)–(6) is discontinuous. This boundary coincides with the outer boundary before time t_0, when the concentration of the dispersed drug drops to 0 at the outer boundary. Typically the inner boundary goes inward and reaches $r = 0$ at time t_*.

The purpose of this work is to develop a fast computational algorithm for solving Eqs. (4)–(6) for the concentration of water and drug, and then predict the drug release behavior described by

the relative drug release $M(t)/M_\infty$, where $M(t)$ and M_∞ denote the volume of drug released at time t and as $t \to \infty$, respectively. In particular,

$$M(t) = \frac{4}{3}\pi R_0^3 C_0 - \int_0^{R(t)} 4\pi r^2 [C_{\mathrm{d}}(r,t) + C_{\mathrm{u}}(r,t)]dr$$

and $M_\infty = \frac{4}{3}\pi R_0^3 C_0$. Therefore, we have

$$\frac{M(t)}{M_\infty} = 1 - \frac{3}{R_0^3 C_0}\int_0^{R(t)} r^2 [C_{\mathrm{d}}(r,t) + C_{\mathrm{u}}(r,t)]dr, \tag{11}$$

which will be used in our numerical computations.

B. Nondimensionalization

When the swelling front is moving, we are not able to find the exact solution analytically. Thus, numerical methods, such as finite element and finite difference methods, come into play. In this article, we discuss multilevel methods to achieve a better approximation with cheaper computational costs compared to traditional methods. We assume the diffusion coefficients are constant for simplification. The methods also work in the case of nonlinear or inhomogeneous diffusion.

We shall now reformulate the governing system of equations in dimensionless variables to make it suitable for numerical computations. Differentiating both sides of Eq. (10) with respect to t, we have

$$\begin{aligned} 4\pi R(t)^2 \frac{dR(t)}{dt} &= \frac{dR(t)}{dt} C_{\mathrm{w}}(R(t),t) 4\pi R(t)^2 + \int_0^{R(t)} 4\pi r^2 \frac{\partial C_{\mathrm{w}}(r,t)}{\partial t} dr \\ &\quad + \frac{dR(t)}{dt}[C_{\mathrm{d}}(R(t),t) + C_{\mathrm{u}}(R(t),t)]4\pi R(t)^2 \\ &\quad + \int_0^{R(t)} 4\pi r^2 \frac{\partial (C_{\mathrm{d}}(r,t) + C_{\mathrm{u}}(r,t))}{\partial t} dr - k_{\mathrm{p}} 4\pi R(t)^2. \end{aligned}$$

Substituting Eqs. (4), (5), (6), and (8) into the above equation, we obtain

$$\left(1 - C_{\mathrm{w,e}} - C_{\mathrm{u}}|_{r=R(t)}\right) \frac{dR(t)}{dt} = D_{\mathrm{w}} \frac{\partial C_{\mathrm{w}}}{\partial r}\bigg|_{r=R(t)} + D_{\mathrm{d}} \frac{\partial C_{\mathrm{d}}}{\partial r}\bigg|_{r=R(t)} - k_{\mathrm{p}}. \tag{12}$$

Let's introduce the following dimensionless variables for convenience,

$$\overline{C}_{\mathrm{w}} = \frac{C_{\mathrm{w}}}{C_{\mathrm{w,e}}} - 1, \quad \overline{C}_{\mathrm{d}} = \frac{C_{\mathrm{d}}}{C_{\mathrm{d,s}}}, \quad \overline{C}_{\mathrm{u}} = \frac{C_{\mathrm{u}}}{C_{\mathrm{d,s}}}, \quad D_{\mathrm{wd}} = \frac{D_{\mathrm{w}}}{D_{\mathrm{d}}},$$

and

$$z = \frac{r}{R_0}, \quad \tau = \frac{t D_{\mathrm{d}}}{R_0^2}, \quad Z(\tau) = \frac{R(t)}{R_0}, \quad \overline{k}_{\mathrm{d}} = \frac{k_{\mathrm{d}} R_0^2}{D_{\mathrm{d}}}, \quad \overline{k}_{\mathrm{p}} = \frac{k_{\mathrm{p}} R_0}{D_{\mathrm{d}}}.$$

Note that C_{w} is scaled to make $\overline{C}_{\mathrm{w}} = 0$ at $z = Z(\tau)$ for any τ. This boundary condition is suitable for the construction of our multilevel schemes.

Thus, the model is transformed to the system of three equations,

$$\frac{\partial \overline{C}_{\rm w}}{\partial \tau} = \frac{D_{\rm wd}}{z^2}\frac{\partial}{\partial z}\left(z^2\frac{\partial \overline{C}_{\rm w}}{\partial z}\right), \tag{13}$$

$$\frac{\partial \overline{C}_{\rm d}}{\partial \tau} = \frac{1}{z^2}\frac{\partial}{\partial z}\left(z^2\frac{\partial \overline{C}_{\rm d}}{\partial z}\right) + \overline{k}_{\rm d}(1-\overline{C}_{\rm d})H(\overline{C}_{\rm u}), \tag{14}$$

$$\frac{\partial \overline{C}_{\rm u}}{\partial \tau} = -\overline{k}_{\rm d}(1-\overline{C}_{\rm d})H(\overline{C}_{\rm u}), \tag{15}$$

supplemented by the initial condition,

$$\tau = 0,\ \ 0 \le z \le 1: \quad \overline{C}_{\rm w} = -1, \quad \overline{C}_{\rm d} = 1, \quad \overline{C}_{\rm u} = \frac{C_0}{C_{\rm d,s}} - 1, \tag{16}$$

and boundary conditions

$$\tau > 0,\ \ z = Z(\tau): \quad \overline{C}_{\rm w} = 0, \quad \overline{C}_{\rm d} = 0, \tag{17}$$

$$\tau > 0,\ \ z = 0: \quad \frac{\partial \overline{C}_{\rm w}}{\partial z} = 0, \quad \frac{\partial \overline{C}_{\rm d}}{\partial z} = 0, \tag{18}$$

and

$$\left(1 - C_{\rm w,e} - C_{\rm d,s}\overline{C}_{\rm u}|_{z=Z(\tau)}\right)\frac{dZ(\tau)}{d\tau} = C_{\rm w,e}D_{\rm wd}\left.\frac{\partial \overline{C}_{\rm w}}{\partial z}\right|_{z=Z(\tau)} + C_{\rm d,s}\left.\frac{\partial \overline{C}_{\rm d}}{\partial z}\right|_{z=Z(\tau)} - \overline{k}_{\rm p}. \tag{19}$$

The system (13)–(15) with initial (16) and boundary (17)–(19) conditions is a starting point for our numerical work.

III. MULTILEVEL COMPUTATIONS

The system of diffusion equations (13)–(15) with initial (16) and boundary (17)–(19) conditions is solved numerically by two methods. The first method uses finite elements, which are conventional numerical tools in the context of the drug delivery problems. The other method is based on the multilevel scheme, which is our main contribution to the subject. The convergence of the finite element method for the diffusion equation (13) with fixed boundary has been studied in Ref. [18].

A. The Finite Element Method

We apply here the finite element method to solve the system of Eqs. (13)–(15) numerically. We only introduce the numerical scheme for solving the diffusion equation (14) with corresponding initial and boundary conditions. The other equations can be handled in the same way without any extra difficulty.

At the discrete time $\tau_i = i\Delta\tau$, $i \in \mathbb{N}_0$, where $\Delta\tau$ is the time step, the domain of the problem is $[0, Z(\tau_i)]$. For a positive integer $n \in \mathbb{N}$ and the uniform partition of $[0, Z(\tau_i)]$, $0 = z^i_{n,0} < z^i_{n,1} < \cdots < z^i_{n,2^n} = Z(\tau_i)$, with $z^i_{n,j} = jZ(\tau_i)/2^n$, $j = 0, \ldots, 2^n$, and $\Delta z^i = Z(\tau_i)/2^n$ we define

$$\phi^i_{n,1}(z) := \phi_b\left(\frac{2^n}{Z(\tau_i)}z - 1\right),$$

and

$$\phi^i_{n,j}(z) := \phi\left(\frac{2^n}{Z(\tau_i)}z - j\right), \quad j = 2, \ldots, 2^n - 1,$$

where

$$\phi_b(z) = \begin{cases} 1 & \text{if} \quad z \in [-1, 0), \\ 1 - z & \text{if} \quad z \in (0, 1], \\ 0 & \text{elsewhere,} \end{cases} \quad \text{and} \quad \phi(z) = \begin{cases} 1 + z & \text{if} \quad z \in [-1, 0), \\ 1 - z & \text{if} \quad z \in (0, 1], \\ 0 & \text{elsewhere.} \end{cases}$$

Here, we consider 2^n elements in the interval $[0, Z(\tau_i)]$, because the dyadic number of elements is suitable for multilevel schemes. The elements are represented by the hat-shaped function ϕ. The function ϕ_b is used to deal with the boundary condition in (18). The boundary condition (17) is automatically accounted by the function ϕ.

Let $\Phi^i_n := \{\phi^i_{n,j}\}_{j=1}^{2^n-1}$ and $V^i_n := \text{span}\{\Phi^i_n\}$. It is easy to see that Φ^i_n is linearly independent. Moreover,

$$\phi^i_{n,1} = \phi^i_{n+1,1} + \phi^i_{n+1,2} + \frac{1}{2}\phi^i_{n+1,3}$$

and

$$\phi^i_{n,j} = \frac{1}{2}\phi^i_{n+1,2j-1} + \phi^i_{n+1,2j} + \frac{1}{2}\phi^i_{n+1,2j+1}, \quad j = 2, \ldots, 2^n - 1,$$

thus we have $V^i_n \subset V^i_{n+1}$ for $n \in \mathbb{N}$. This relation is crucial, because we need to construct complementary subspace W^i_n of V^i_n in V^i_{n+1} to propose our multilevel scheme.

The Galerkin method is to seek

$$\overline{C}^i_{\mathrm{d}} := \overline{C}_{\mathrm{d}}(z, \tau_i) = \sum_{j=1}^{2^n-1} x^i_{n,j}\phi^i_{n,j}(z)$$

satisfying for $j = 1, 2, \ldots, 2^n - 1$,

$$\int_0^{Z(\tau_i)} z^2 \left[\frac{\partial \overline{C}_{\mathrm{d}}}{\partial \tau}\phi^i_{n,j} + \frac{\partial \overline{C}_{\mathrm{d}}}{\partial z}(\phi^i_{n,j})' + \overline{k}_{\mathrm{d}}\overline{C}_{\mathrm{d}}H(\overline{C}_{\mathrm{u}})\phi^i_{n,j}\right] dz = \overline{k}_{\mathrm{d}}\int_0^{Z(\tau_i)} z^2 H(\overline{C}_{\mathrm{u}})\phi^i_{n,j}\, dz$$

Next, we use the backward Euler method for discretization with respect to the time variable τ. This method is defined by replacing the time derivative by a backward difference quotient and leads to solving a sequence of matrix equations,

$$E^i_n x^i_n = \xi^i_n, \quad i \in \mathbb{N}, \tag{20}$$

where

$$E^i_n = A^i_n + \Delta\tau B^i_n + \Delta\tau\overline{k}_{\mathrm{d}}G^i_n$$

with

$$A^i_n = \left(\int_0^{Z(\tau_i)} z^2\sigma\phi\, dz\right)_{\sigma,\phi\in\Phi^i_n}, \quad B^i_n = \left(\int_0^{Z(\tau_i)} z^2\sigma'\phi'\, dz\right)_{\sigma,\phi\in\Phi^i_n},$$

and

$$G_n^i = \left(\int_0^{Z(\tau_i)} z^2 H(\overline{C}_{\rm u}^{i-1}) \sigma \phi dz \right)_{\sigma,\phi \in \Phi_n^i}.$$

Here $x_n^i = (x_\phi)_{\phi \in \Phi_n^i}$ and

$$\xi_n^i = \left(\Delta\tau \overline{k}_{\rm d} \int_0^{Z(\tau_i)} z^2 H(\overline{C}_{\rm u}^{i-1}) \phi dz \right)_{\phi \in \Phi_n^i} + H_n^i x_n^{i-1},$$

where $H_n^i = \left(\int_0^{Z(\tau_i)} z^2 \sigma \phi dz \right)_{\sigma \in \Phi_n^i, \phi \in \Phi_n^{i-1}}$.

Finally, we have to calculate the moving boundary position $Z(\tau_i)$. We use the following difference scheme to discretize the differential equation (19):

$$\begin{aligned} &\left(1 - C_{\rm w,e} - C_{\rm d,s} \overline{C}_{\rm u}^{i-1}(z_{n,2^n}^{i-1})\right) \frac{Z(\tau_i) - Z(\tau_{i-1})}{\Delta\tau} \\ &\quad = C_{\rm w,e} D_{\rm wd} \frac{\overline{C}_{\rm w}^{i-1}(z_{n,2^n}^{i-1}) - \overline{C}_{\rm w}^{i-1}(z_{n,2^n-1}^{i-1})}{\Delta z^{i-1}} + C_{\rm d,s} \frac{\overline{C}_{\rm d}^{i-1}(z_{n,2^n}^{i-1}) - \overline{C}_{\rm d}^{i-1}(z_{n,2^n-1}^{i-1})}{\Delta z^{i-1}} - \overline{k}_{\rm p}. \end{aligned} \tag{21}$$

This explicit scheme was introduced by Murray and Carey [19]. By using this equation, we are able to track the boundary position $Z(\tau_i)$ from data at the previous time τ_{i-1}. There are many other strategies to deal with the moving boundary in the literature. For example, a predictor-corrector method was also discussed in Ref. [19], where the two methods were analyzed and compared. It turns out that, to achieve equivalent accuracy, larger time steps can be taken with the predictor–corrector method. However, the predictor–corrector method requires more computational efforts per each step. We choose the explicit scheme (21) for simplicity and take the time steps not so large. The algorithm works well using the explicit scheme.

In summary, the computational algorithm using the finite element method for solving the system of diffusion equations (13)–(15) with initial (16) and boundary (17)–(19) conditions is outlined as follows.

Step 1 Set n, $\Delta\tau$, $\tau_0 = 0$ and $Z(\tau_0) = 1$. Set $\overline{C}_{\rm w}^0$, $\overline{C}_{\rm d}^0$ and $\overline{C}_{\rm u}^0$ using the initial condition. In particular, write $\overline{C}_{\rm w}^0$, $\overline{C}_{\rm d}^0$ and $\overline{C}_{\rm u}^0$ as linear combinations of the basis functions in Φ_n^0, respectively, according to (16).

Step 2 For $i = 1, 2, \ldots$,

- **2.1** $\tau_i = \tau_{i-1} + \Delta\tau$.
- **2.2** Solve the difference equation (21) for $Z(\tau_i)$.
- **2.3** Divide the interval $[0, Z(\tau_i)]$ into 2^n subintervals with equal length, use the finite element basis Φ_n^i and backward Euler method to discretize equation (14), solve the resulting linear system (20) by the conjugate gradient (CG) method and obtain $\overline{C}_{\rm d}^i$. Obtain $\overline{C}_{\rm w}^i$ and $\overline{C}_{\rm u}^i$ in a similar way.

Step 3 Stop when $\overline{C}_{\rm d}^i = 0$.

Here, we do not use the front-fixing method, which was proposed by Landau [20] and applied to moving boundary problems in controlled drug release [2, 10]. By introducing a variable $\eta = z/Z(\tau)$, the computational domain is mapped to the unit interval in the front-fixing

method. However, this technique adds first-order derivative terms with respect to variable η with complicated variable coefficients. The cost of dealing with these additional terms in numerical computations may be comparable to the cost of updating the finite elements according to the moving boundary. More importantly, these additional terms make the resulting linear systems to be nonsymmetric, and it is more challenging to develop efficient algorithms for nonsymmetric systems. In addition, it is not easy to extend the front-fixing method to a higher dimensional case.

B. The Multilevel Scheme

The reason we use the backward Euler method instead of the explicit methods is that the stability requirements of the latter impose stringent conditions on the time step size. However, when the time step size is large, the stiffness matrix B_n^i dominates. Its condition number dramatically increases as the level n increases, so does the condition number of E_n^i. This will be explained in details in Section IIIC. Hence, the computational cost of a numerical solution of the matrix system (20) is expensive. To achieve a better approximation with lower computational costs, we follow the idea in Ref. [21] to construct a multilevel basis in V_n^i, which replaces the basis Φ_n^i and improves the condition number of the resulting linear system.

For $n \in \mathbb{N}_0$, we define

$$\psi_{n,1}^i = \frac{1}{\sqrt{Z(\tau_i)}} 2^{n/2+1/2} \phi_{n+1,1}^i$$

and

$$\psi_{n,j}^i = \frac{1}{\sqrt{Z(\tau_i)}} 2^{n/2-k} \phi_{n+1,2j-1}^i \quad \text{for} \quad 2^{k-1}+1 \le j \le 2^k \quad \text{and} \quad k = 1, 2, \ldots, n.$$

Let $\Gamma_n^i := \{\psi_{n,j}^i\}_{j=1}^{2^n}$ and $W_n^i := \text{span}\{\Gamma_n^i\}$. It is easy to see that

$$V_{n+1}^i = V_n^i + W_n^i, \quad n \in \mathbb{N}.$$

Consequently, for any positive integer n, we have

$$V_n^i = W_0^i + W_1^i + \cdots + W_{n-1}^i$$

and $\Psi_n^i := \bigcup_{k=0}^{n-1} \Gamma_k^i$ is a basis of V_n^i other than Φ_n^i. Note that Φ_n^i and Ψ_n^i are two bases of V_n^i, there exists a unique invertible matrix transformation S_n^i such that

$$\Psi_n^i = S_n^i \Phi_n^i.$$

Applying the basis Ψ_n^i instead of Φ_n^i, we obtain a sequence of matrix system,

$$F_n^i y_n^i = \eta_n^i, \quad i \in \mathbb{N}, \tag{22}$$

where

$$F_n^i = \bar{A}_n^i + \Delta\tau \bar{B}_n^i + \Delta\tau \bar{k}_{\text{d}} \bar{G}_n^i$$

with

$$\bar{A}_n^i = \left(\int_0^{Z(\tau_i)} z^2 \chi \psi \, dz \right)_{\chi,\psi \in \Psi_n^i}, \quad \bar{B}_n^i = \left(\int_0^{Z(\tau_i)} z^2 \chi' \psi' \, dz \right)_{\chi,\psi \in \Psi_n^i},$$

and

$$\bar{G}_n^i = \left(\int_0^{Z(\tau_i)} z^2 H(\overline{C}_{\rm u}^{i-1}) \chi \psi dz \right)_{\chi,\psi \in \Psi_n^i}.$$

Here $y_n^i = \left(y_\psi\right)_{\psi \in \Psi_n^i}$ and

$$\eta_n^i = \left(\Delta\tau \overline{k}_{\rm d} \int_0^{Z(\tau_i)} z^2 H(\overline{C}_{\rm u}^{i-1}) \psi dz \right)_{\psi \in \Psi_n^i} + \bar{H}_n^i y_n^{i-1},$$

where $\bar{H}_n^i = \left(\int_0^{Z(\tau_i)} z^2 \chi \psi dz \right)_{\chi \in \Psi_n^i, \psi \in \Psi_n^{i-1}}$.

It follows from explicit expressions that

$$\bar{A}_n^i = S_n^i A_n^i (S_n^i)^T, \quad \bar{B}_n^i = S_n^i B_n^i (S_n^i)^T, \quad \bar{G}_n^i = S_n^i G_n^i (S_n^i)^T, \quad \eta_n^i = S_n^i \xi_n.$$

Consequently $F_n^i = S_n^i E_n^i (S_n^i)^T$, hence, the system (22) is equivalent to

$$S_n^i E_n^i (S_n^i)^T y_n^i = S_n^i \xi_n^i. \tag{23}$$

Because A_n^i, B_n^i, and G_n^i are symmetric and positive definite, so are E_n^i and $S_n^i E_n^i (S_n^i)^T$ as $\Delta\tau$ and $\overline{k}_{\rm d}$ are positive. If the condition number of $S_n^i E_n^i (S_n^i)^T$ is uniformly bounded (independent of n), the linear system (23) can be solved by the CG method. The number of iterations needed to achieve the same accuracy at each time step is independent of n. Although the CG method for solving (23) is equivalent to the preconditioned CG (PCG) method for solving (20), it has a higher computational cost. Therefore, we will apply PCG to solve (20) with preconditioner S_n^i. Consequently, the computational algorithm using the multilevel scheme for solving the system of diffusion equations (13)–(15) with initial (16) and boundary (17)–(19) conditions is obtained by replacing the CG method with the PCG method, using the preconditioner S_n^i constructed in this section.

C. Stability Analysis

We prove here that S_n^i is a good preconditioner for E_n^i for fixed i and time step $\Delta\tau$. In other words, we show that for fixed i and $\Delta\tau$, the condition number of $S_n^i E_n^i (S_n^i)^T$ is uniformly bounded as $n \to \infty$. Our proof is motivated by the techniques used in Ref. [21]. Recall that, for a symmetric positive definite matrix A, its condition number is given by

$$\kappa(A) = \frac{\lambda_{\max,A}}{\lambda_{\min,A}},$$

where $\lambda_{\max,A}$ and $\lambda_{\min,A}$ stands for the maximal and minimal eigenvalues of A, respectively.

Lemma 3.1. *For any $x \in \mathbb{R}^{2^n-1}$, we have*

$$\Delta\tau x^T B_n^i x \le x^T E_n^i x \le \mu_i \Delta\tau x^T B_n^i x, \quad \mu_i = 1 + \frac{4(1+\Delta\tau\overline{k}_{\rm d})}{9\Delta\tau} (Z(\tau_i))^2.$$

Proof. Suppose $x = (x_1, x_2, \ldots, x_{2^n-1})^T \in \mathbb{R}^{2^n-1}$ and let $f = \sum_{j=1}^{2^n-1} x_j \phi_{n,j}^i$. We have

$$\int_0^{Z(\tau_i)} z^2 f^2 dz \le \frac{4}{9}(Z(\tau_i))^2 \int_0^{Z(\tau_i)} z^2 |f'|^2 dz. \tag{24}$$

Indeed,

$$\begin{aligned}
\int_0^{Z(\tau_i)} z^2 f^2 dz &= \int_0^{Z(\tau_i)} z^2 f^2 dz \\
&= \frac{1}{3} z^3 f^2 \Big|_0^{Z(\tau_i)} - \frac{2}{3} \int_0^{Z(\tau_i)} z^3 f f' dz \\
&\le \frac{2}{3} \int_0^{Z(\tau_i)} Z(\tau_i) \left| z f z f' \right| dz \\
&\le \frac{2}{3} Z(\tau_i) \left(\int_0^{Z(\tau_i)} z^2 f^2 dz \right)^{1/2} \left(\int_0^{Z(\tau_i)} z^2 |f'|^2 dz \right)^{1/2}.
\end{aligned}$$

Squaring both sides and dividing by $\int_0^{Z(\tau_i)} z^2 f^2 dz$, we obtain (24). Note that

$$\begin{aligned}
x^T E_n^i x &= x^T A_n^i x + \Delta\tau x^T B_n^i x + \Delta\tau \overline{k}_{\mathrm{d}} x^T G_n^i x \\
&= \int_0^{Z(\tau_i)} z^2 f^2 dz + \Delta\tau \int_0^{Z(\tau_i)} z^2 |f'|^2 dz + \Delta\tau \overline{k}_{\mathrm{d}} \int_0^{Z(\tau_i)} z^2 H(\overline{C}_{\mathrm{u}}^{i-1}) f^2 dz.
\end{aligned}$$

Thus, on one hand,

$$x^T E_n^i x \ge \Delta\tau \int_0^{Z(\tau_i)} z^2 |f'|^2 dz = \Delta\tau x^T B_n^i x.$$

On the other hand,

$$\begin{aligned}
x^T E_n^i x &\le \int_0^{Z(\tau_i)} z^2 f^2 dz + \Delta\tau \int_0^{Z(\tau_i)} z^2 |f'|^2 dz + \Delta\tau \overline{k}_{\mathrm{d}} \int_0^{Z(\tau_i)} z^2 f^2 dz \\
&= (1 + \Delta\tau \overline{k}_{\mathrm{d}}) \int_0^{Z(\tau_i)} z^2 f^2 dz + \Delta\tau \int_0^{Z(\tau_i)} z^2 |f'|^2 dz \\
&\le \left(\frac{4}{9}(Z(\tau_i))^2 (1 + \Delta\tau \overline{k}_{\mathrm{d}}) + \Delta\tau \right) x^T B_n^i x.
\end{aligned}$$

The last inequality is obtained using (24). ∎

For any eigenvalue $\lambda_{B_n^i}$ of B_n^i, there exists a column vector x such that

$$\lambda_{B_n^i} = \frac{x^T B_n^i x}{x^T x}.$$

From Lemma 3.1, we have

$$\frac{\lambda_{\min, E_n^i}}{\mu_i \Delta\tau} \le \frac{1}{\mu_i \Delta\tau} \frac{x^T E_n^i x}{x^T x} \le \lambda_{B_n^i} \le \frac{1}{\Delta\tau} \frac{x^T E_n^i x}{x^T x} \le \frac{\lambda_{\max, E_n^i}}{\Delta\tau}.$$

Therefore, we have $\kappa(E_n^i) \geq \kappa(B_n^i)/\mu_i$. As the condition number of the matrix B_n^i increases dramatically as n increases [22], so does the condition number of E_n^i for fixed i and $\Delta\tau$.

To show that S_n^i is a good preconditioner of E_n^i, we only need to show $S_n^i B_n^i (S_n^i)^T$ is well-conditioned. In the following, we first construct a matrix $\widetilde{B}_n^i$ such that $\kappa(S_n^i B_n^i (S_n^i)^T)$ can be controlled by $\kappa(S_n^i \widetilde{B}_n^i (S_n^i)^T)$ multiplied by a constant, and then verify that $\kappa(S_n^i \widetilde{B}_n^i (S_n^i)^T)$ is uniformly bounded as $n \to \infty$.

Let

$$w_n^i := \sum_{k=1}^{n} 2^{-k} Z(\tau_i) \chi_{[2^{-k} Z(\tau_i), 2^{-k+1} Z(\tau_i)]} \quad \text{and} \quad u_{n,j}^i := w_n^i (\phi_{n,j}^i)',$$

where χ is the characteristic function. Define $\widetilde{\Phi}_n^i := \{u_{n,j}^i\}_{j=1}^{2^n-1}$ and $\widetilde{V}_n^i := \text{span}\{\widetilde{\Phi}_n^i\}$. It is easy to check that $\widetilde{\Phi}_n^i$ is linearly independent. Moreover, we have

$$u_{n,1}^i = u_{n+1,1}^i + u_{n+1,2}^i + \frac{1}{2} u_{n+1,3}^i$$

and

$$u_{n,j}^i = \frac{1}{2} u_{n+1,2j-1}^i + u_{n+1,2j}^i + \frac{1}{2} u_{n+1,2j+1}^i, \quad j = 2, \ldots, 2^n - 1,$$

almost everywhere. Thus, we have $\widetilde{V}_n^i \subset \widetilde{V}_{n+1}^i$ for $n \in \mathbb{N}$. We shall now define $\widetilde{B}_n^i = (\widetilde{b}_{jk}^i)_{1 \leq j,k \leq 2^n-1}$ and $\widetilde{b}_{jk}^i = \int_0^{Z(\tau_i)} u_{n,j}^i u_{n,k}^i dz$.

Lemma 3.2. *For any $x \in \mathbb{R}^{2^n-1}$, we have*

$$x^T \widetilde{B}_n^i x \leq x^T B_n^i x \leq 4 x^T \widetilde{B}_n^i x.$$

Proof. Suppose $x = (x_1, x_2, \ldots, x_{2^n-1})^T \in \mathbb{R}^{2^n-1}$ and denote

$$f = \sum_{j=1}^{2^n-1} x_j \phi_{n,j}^i \quad \text{and} \quad g = \sum_{j=1}^{2^n-1} x_j u_{n,j}^i.$$

By the definition of $\phi_{n,j}^i$, it is easy to see that $f' = 0$ and $g = 0$ on $(0, 2^{-n} Z(\tau_i))$. Then, we have

$$\begin{aligned}
x^T B_n^i x &= \int_0^{Z(\tau_i)} z^2 |f'|^2 dz = \int_{2^{-n} Z(\tau_i)}^{Z(\tau_i)} z^2 |f'|^2 dz \\
&= \int_{2^{-n} Z(\tau_i)}^{Z(\tau_i)} z^2 \left| \sum_{j=1}^{2^n-1} x_j (\phi_{n,j}^i)' \right|^2 dz \\
&= \sum_{k=1}^{n} \int_{2^{-k} Z(\tau_i)}^{2^{-k+1} Z(\tau_i)} z^2 \left| \sum_{j=1}^{2^n-1} x_j (\phi_{n,j}^i)' \right|^2 dz \\
&\leq \sum_{k=1}^{n} \int_{2^{-k} Z(\tau_i)}^{2^{-k+1} Z(\tau_i)} (2^{-k+1} Z(\tau_i))^2 \left| \sum_{j=1}^{2^n-1} x_j (\phi_{n,j}^i)' \chi_{[2^{-k} Z(\tau_i), 2^{-k+1} Z(\tau_i)]} \right|^2 dz
\end{aligned}$$

$$
\begin{aligned}
&= 4\sum_{k=1}^{n}\int_{2^{-k}Z(\tau_i)}^{2^{-k+1}Z(\tau_i)}\left|\sum_{j=1}^{2^n-1}x_j 2^{-k}Z(\tau_i)\chi_{[2^{-k}Z(\tau_i),2^{-k+1}Z(\tau_i)]}(\phi_{n,j}^i)'\right|^2 dz\\
&= 4\sum_{k=1}^{n}\int_{2^{-k}Z(\tau_i)}^{2^{-k+1}Z(\tau_i)}\left|\sum_{j=1}^{2^n-1}x_j w_n^i(\phi_{n,j}^i)'\right|^2 dz\\
&= 4\sum_{k=1}^{n}\int_{2^{-k}Z(\tau_i)}^{2^{-k+1}Z(\tau_i)}\left|\sum_{j=1}^{2^n-1}x_j u_{n,j}^i\right|^2 dz\\
&= 4\int_{2^{-n}Z(\tau_i)}^{Z(\tau_i)}|g|^2dz = 4\int_{0}^{Z(\tau_i)}|g|^2dz\\
&= 4x^T\widetilde{B}_n^i x.
\end{aligned}
$$

Similarly,

$$
x^T B_n^i x \geq \sum_{k=1}^{n}\int_{2^{-k}Z(\tau_i)}^{2^{-k+1}Z(\tau_i)}(2^{-k}Z(\tau_i))^2\left|\sum_{j=1}^{2^n-1}x_j(\phi_{n,j}^i)'\chi_{[2^{-k}Z(\tau_i),2^{-k+1}Z(\tau_i)]}\right|^2 dz = x^T\widetilde{B}_n^i x.
$$

This completes the proof. ∎

Next, we show that $\kappa(S_n^i\widetilde{B}_n^i(S_n^i)^T)$ is uniformly bounded as $n\to\infty$. For $n\in\mathbb{N}_0$, similar to the definition of $\psi_{n,j}^i$, we define

$$
v_{n,1}^i = \frac{1}{\sqrt{Z(\tau_i)}}2^{n/2+1/2}u_{n+1,1}^i
$$

and

$$
v_{n,j}^i = \frac{1}{\sqrt{Z(\tau_i)}}2^{n/2-k}u_{n+1,2j-1}^i \quad \text{for} \quad 2^{k-1}+1\leq j\leq 2^k \quad \text{and} \quad k=1,2,\ldots,n.
$$

Let $\widetilde{\Gamma}_n^i := \{v_{n,j}^i\}_{j=1}^{2^n}$ and $\widetilde{W}_n^i := \operatorname{span}\{\widetilde{\Gamma}_n^i\}$. It is easy to see that

$$
\widetilde{V}_{n+1}^i = \widetilde{V}_n^i + \widetilde{W}_n^i, \quad n\in\mathbb{N}.
$$

Consequently, for any positive integer n, we have

$$
\widetilde{V}_n^i = \widetilde{W}_0^i + \widetilde{W}_1^i + \cdots + \widetilde{W}_{n-1}^i
$$

and $\widetilde{\Psi}_n^i := \bigcup_{k=0}^{n-1}\widetilde{\Gamma}_k^i$ is a basis of $\widetilde{V}_n^i$ other than $\widetilde{\Phi}_n^i$. From the definition, we have $\widetilde{\Psi}_n^i = S_n^i\widetilde{\Phi}_n^i$ and

$$
S_n^i\widetilde{B}_n^i(S_n^i)^T = S_n^i\left(\int_0^{Z(\tau_i)}uvdz\right)_{u,v\in\widetilde{\Phi}_n^i}(S_n^i)^T = \left(\int_0^{Z(\tau_i)}uvdz\right)_{u,v\in\widetilde{\Psi}_n^i}.
$$

We use this formula to prove the following.

Lemma 3.3. *$S_n^i \widetilde{B}_n^i (S_n^i)^T$ is a $(2^n-1)\times(2^n-1)$ identity matrix.*

Proof. To prove the lemma, we show that $\widetilde{\Psi}_n^i$ is an orthonormal basis of $\widetilde{V}_n^i$.

First, we show that $\widetilde{V}_l^i$ and $\widetilde{W}_l^i$ are orthogonal with respect to the inner product in L^2 for any $l \in \mathbb{N}$. Indeed, $v_{l,1}^i$ is orthogonal to $u_{l,j'}^i$ for any $j' = 1, \ldots, 2^l - 1$, because their supports do not overlap. For $j = 2, \ldots, 2^l$, there exists k such that $2^{k-1} + 1 \le j \le 2^k$ and, by definition, we have

$$v_{l,j}^i = \frac{1}{\sqrt{Z(\tau_i)}} 2^{l/2-k} u_{l+1,2j-1}^i = \begin{cases} \dfrac{1}{\sqrt{Z(\tau_i)}} 2^{l/2}, & x \in \left(\dfrac{2j-2}{2^{l+1}} Z(\tau_i), \dfrac{2j-1}{2^{l+1}} Z(\tau_i) \right), \\ -\dfrac{1}{\sqrt{Z(\tau_i)}} 2^{l/2}, & x \in \left(\dfrac{2j-1}{2^{l+1}} Z(\tau_i), \dfrac{2j}{2^{l+1}} Z(\tau_i) \right), \\ 0, & \text{elsewhere.} \end{cases}$$

We can see that the support of $v_{l,j}^i$ is $[\frac{j-1}{2^l} Z(\tau_i), \frac{j}{2^l} Z(\tau_i)]$ and the integral of $v_{l,j}^i$ on this interval is zero. Because $u_{l,j'}^i$ for any $j' = 1, \ldots, 2^l - 1$ is a constant inside this interval, $v_{l,j}^i$ is orthogonal to $u_{l,j'}^i$ for any $j = 2, \ldots, 2^l$ and $j' = 1, \ldots, 2^l - 1$.

Second, we show that $v_{l,j}^i$ is orthogonal to $v_{l,j'}^i$ for any $1 \le j, j' \le 2^l$ and $j \ne j'$. This is so because their supports do not overlap.

Finally, we establish the normalization conditions for $v_{l,j}^i$. For any $j = 2, \ldots, 2^l$, there exists k such that $2^{k-1} + 1 \le j \le 2^k$, then

$$\int_0^{Z(\tau_i)} |v_{l,j}^i|^2 dz = \int_{\frac{2j-2}{2^{l+1}} Z(\tau_i)}^{\frac{2j-1}{2^{l+1}} Z(\tau_i)} \frac{1}{Z(\tau_i)} 2^l dz + \int_{\frac{2j-1}{2^{l+1}} Z(\tau_i)}^{\frac{2j}{2^{l+1}} Z(\tau_i)} \frac{1}{Z(\tau_i)} 2^l dz = 1.$$

For $j = 1$, we have

$$v_{l,1}^i = \frac{1}{\sqrt{Z(\tau_i)}} 2^{l/2+1/2} u_{l+1,1}^i = \begin{cases} -\frac{1}{\sqrt{Z(\tau_i)}} 2^{l/2+1/2}, & x \in (\frac{2j-1}{2^{l+1}} Z(\tau_i), \frac{2j}{2^{l+1}} Z(\tau_i)), \\ 0, & \text{elsewhere,} \end{cases}$$

and hence,

$$\int_0^{Z(\tau_i)} |v_{l,1}^i|^2 dz = \int_{\frac{1}{2^{l+1}} Z(\tau_i)}^{\frac{2}{2^{l+1}} Z(\tau_i)} \frac{1}{Z(\tau_i)} 2^{l+1} dz = 1.$$

Therefore, for any $u, v \in \widetilde{\Psi}_n^i$,

$$\int_0^{Z(\tau_i)} uv dz = \begin{cases} 1, & u = v, \\ 0, & u \ne v. \end{cases}$$

The assertion of the lemma is proved. ∎

Based on the three lemmas above, we have the following theorem.

Theorem 3.4. *Given the time step $\Delta\tau$, for any $i = 1, 2, \ldots$, we have $\kappa(S_n^i E_n^i (S_n^i)^T) \le 4\mu_i$.*

Proof. According to the above lemmas, for any column vector x of size $(2^n - 1)$, on one hand,

$$\begin{aligned} x^T S_n^i E_n^i (S_n^i)^T x &= [(S_n^i)^T x]^T E_n^i [(S_n^i)^T x] \le \Delta\tau\mu_i [(S_n^i)^T x]^T B_n^i [(S_n^i)^T x] \\ &\le 4\Delta\tau\mu_i [(S_n^i)^T x]^T \widetilde{B}_n^i [(S_n^i)^T x] \\ &= 4\Delta\tau\mu_i x^T x. \end{aligned}$$

On the other side,

$$\begin{aligned} x^T S_n^i E_n^i (S_n^i)^T x &= [(S_n^i)^T x]^T E_n^i [(S_n^i)^T x] \ge \Delta\tau [(S_n^i)^T x]^T B_n^i [(S_n^i)^T x] \ge \Delta\tau [(S_n^i)^T x]^T \widetilde{B}_n^i [(S_n^i)^T x] \\ &= \Delta\tau x^T x. \end{aligned}$$

For any eigenvalue λ of $S_n^i E_n^i (S_n^i)^T$, there exists a vector x such that

$$\lambda = \frac{x^T S_n^i E_n^i (S_n^i)^T x}{x^T x}.$$

Thus $\lambda \in [\Delta\tau, \Delta\tau\mu_i]$. Consequently,

$$\kappa(S_n^i E_n^i (S_n^i)^T) = \frac{\lambda_{\max, S_n^i E_n^i (S_n^i)^T}}{\lambda_{\min, S_n^i E_n^i (S_n^i)^T}} \le 4\mu_i,$$

which proves the assertion of the theorem. ∎

In Theorem 3.4, the upper bound is independent of n, thus the condition number of $S_n^i E_n^i (S_n^i)^T$ is uniformly bounded as $n \to \infty$.

IV. NUMERICAL RESULTS AND COMPARISON

We compare performance of the finite element and multilevel schemes in numerical simulations of the system of diffusion equations (13)–(15) supplemented by initial (16) and boundary (17)–(19) conditions. We first solve the system numerically up to time τ to obtain the concentration of water, dissolved drug, and dispersed drug at τ. Then, we can use Eq. (11) to obtain the relative drug release. In our numerical computation, we choose the following values for the parameters appearing in the model,

$$R_0 = 0.1 \text{ cm}, \quad C_0 = 3C_{\text{d,s}}, \quad D_{\text{w}} = 2.9 \times 10^{-6} \text{ cm}^2\text{s}^{-1}, \quad D_{\text{d}} = 1.5 \times 10^{-6} \text{ cm}^2\text{s}^{-1},$$
$$\overline{k}_{\text{d}} = 3.448, \quad C_{\text{d,s}} = 0.01, \quad C_{\text{w,e}} = 0.3, \quad \overline{k}_{\text{p}} = 6.11 \times 10^{-3}.$$

These values have been used by pharmaceutical researchers [2,5]. Both the finite element method and the multilevel scheme give the same results but the latter one performs much faster.

Figure 2 illustrates distribution of the concentrations in the drug delivery system at different times, $t = 1, 8, 28, 78$ min. In particular, Fig. 2A gives the dimensionless concentration of the water. We see that as time evolves, the water concentration becomes higher and higher because of water penetration. Figure 2(B,C) show that the concentrations of dissolved drug and dispersed drug decrease as drug diffuses out and dissolves, respectively. Figure 2D provides the total drug

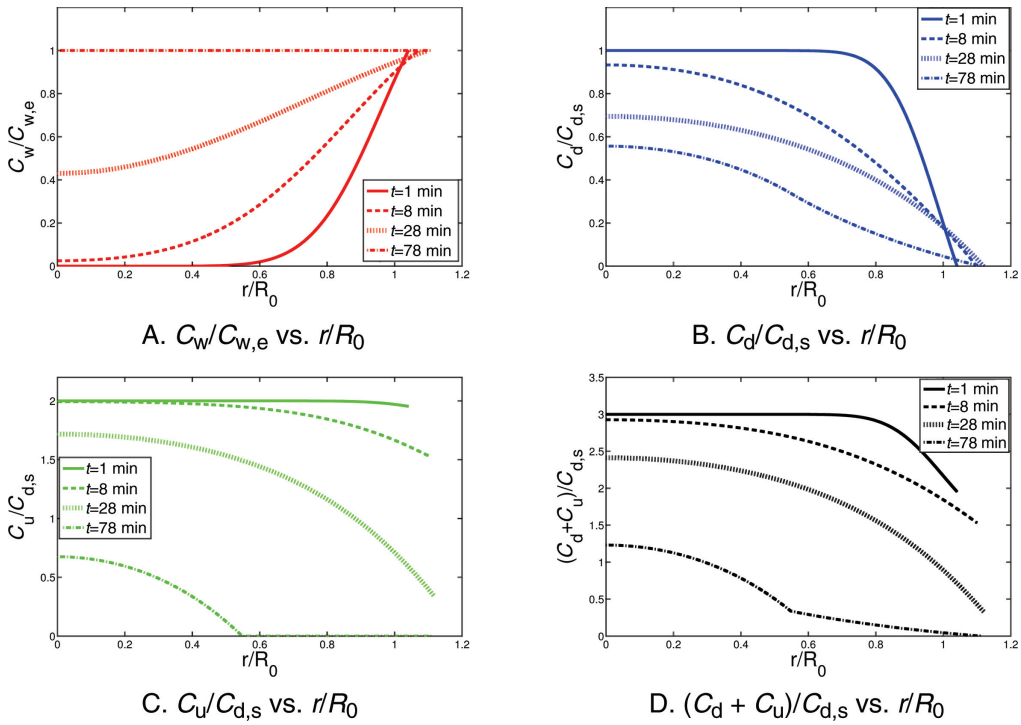

FIG. 2. Concentrations versus radius at different times. [Color figure can be viewed in the online issue, which is available at wileyonlinelibrary.com.]

concentration. In Fig. 2C, the dispersed drug concentration is positive everywhere in the matrix at $t = 1, 8, 28$ min. However, this concentration is zero near the outer boundary at $t = 78$ min. Because of this difference, we may also notice that, in Fig. 2(B,D), the curves at $t = 78$ min looks different from the other three.

Figure 3A depicts how the boundary of the drug release system (outer boundary) and the boundary of dispersed drug (inner boundary) move in time. We see that the outer boundary first moves outward because of polymer swelling. As the polymer approaches its fully swollen status, polymer erosion prevails, which causes the boundary to decrease. Moreover, the inner boundary first coincides with the outer boundary. At time t_0, it separates from the outer boundary, goes inward, and reaches 0 at time t_*. Figure 3B gives the relative drug release in time which describes the drug release behavior. The separation of the inner and outer boundaries results in the change in slope of $M(\tau)$ near 0.3.

A. Comparison of the Finite Element and Multilevel Methods

Although the finite element and multilevel schemes give the same results, they require different computational efforts. To compare their performance, we solve the same problem by these two methods. For the finite element method, the CG algorithm is applied to solve the linear system (20) at each time step. For the multilevel scheme, we solve the same system by the PCG algorithm with preconditioner S_n^i at each time step. The concentration of water, dispersed and dissolved drugs can be obtained similarly by these two methods. We set the threshold to be 10^{-8} in both

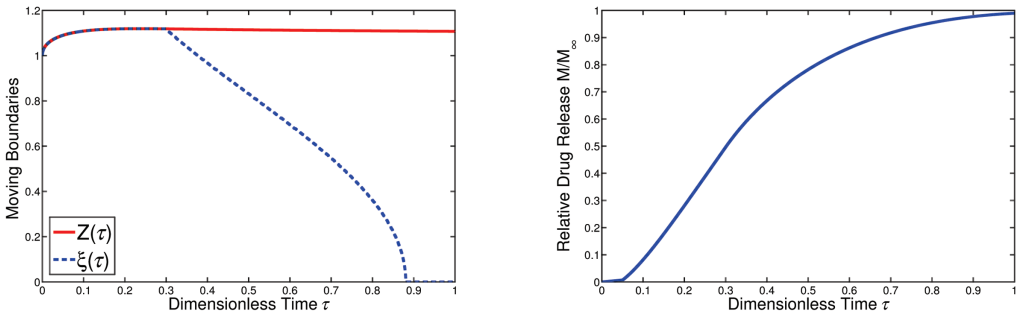

A. $Z(\tau)$ and $\xi(\tau)$ vs. τ B. $M(\tau)/M_\infty$ vs. τ

FIG. 3. Moving boundaries and relative drug release versus time. [Color figure can be viewed in the online issue, which is available at wileyonlinelibrary.com.]

algorithms and compare the number of iterations needed to achieve this accuracy. In particular, the problem is solved up to 2300 s, which yields $\tau = 0.345$ after rescaling.

The parameters in the model are given above. For different time step size $\Delta\tau$ and different level n, the number of CG and PCG iterations needed for solving the linear equation (14) for dissolved drug is listed inside and outside the brackets in Table I, respectively. Table II lists the number of iterations for solving the linear equation (13) for water concentration. We note that the tables list the number of iterations needed at the last time step of numerical computations.

We see that the number of iterations in the multilevel scheme is much less than that needed for the finite element method. For fixed time step size $\Delta\tau$, as the level n increases, the number of CG iterations increases rapidly. However, the number of PCG iterations remains nearly the same. This shows that the multilevel method is well-conditioned, and its condition number is uniformly bounded for larger values of n. Moreover, for fixed level n, as time step size increases, the number of CG iterations increases, but the number of PCG iterations decreases. This is reasonable, because as time step size increases, the linear system (20) becomes more and more ill-conditioned. At the same time, the multilevel method has additional advantages when the time step size increases.

TABLE I. Number of iterations by the multilevel and finite element (in the parentheses) schemes for dissolved drug.

	$n = 8$	$n = 9$	$n = 10$
$\Delta\tau = 0.003$	14 (761)	13 (1807)	13 (4211)
$\Delta\tau = 0.0015$	16 (538)	15 (1308)	14 (2965)
$\Delta\tau = 0.00075$	21 (354)	19 (811)	17 (1711)

TABLE II. Number of iterations by the multilevel and the finite element (in the parentheses) schemes for water.

	$n = 8$	$n = 9$	$n = 10$
$\Delta\tau = 0.003$	16 (752)	20 (1921)	20 (4682)
$\Delta\tau = 0.0015$	19 (710)	22 (1777)	21 (4129)
$\Delta\tau = 0.00075$	25 (537)	28 (1243)	23 (2629)

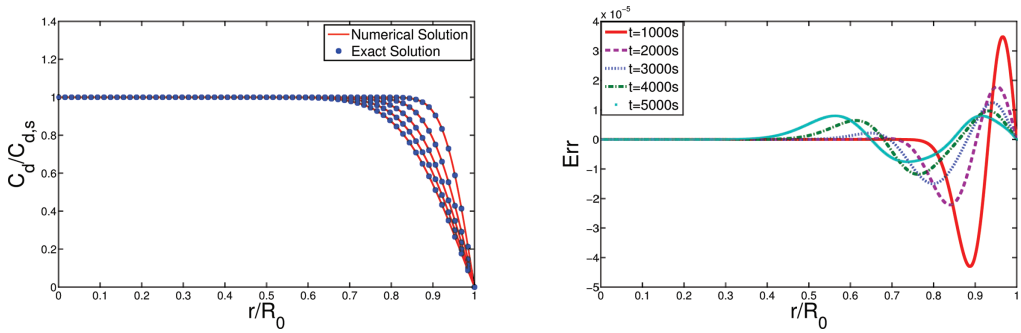

FIG. 4. Left: the numerical and exact solutions for a scalar diffusion equation for $C_{\rm d}/C_{\rm d,s}$ on $[0, t_0]$ in the case of no water and polymer erosion. Right: The distance between the two solutions. [Color figure can be viewed in the online issue, which is available at wileyonlinelibrary.com.]

B. Comparison of Numerical and Exact Solutions

In all future computations, we will omit water and neglect polymer swelling and erosion.

Because the system of diffusion equations (5)–(6) is nonlinear, it is impossible to derive an exact solution. However, if we only consider the time interval $[0, t_0]$, when $C_{\rm u} > 0$ everywhere, the exact solution can be obtained by the method of separation of variables. Appendix A gives details of this exact solution.

The exact solutions for the dimensionless dissolved drug concentration $C_{\rm d}/C_{\rm d,s}$ at different times, $t = 1000\,{\rm s}, 2000\,{\rm s}, 3000\,{\rm s}, 4000\,{\rm s}$, and $5000\,{\rm s}$, follow from Eq. (34). As the condition $C_{\rm u} > 0$ is only valid for a short time interval $[0, t_0]$, these exact solutions can only be used to verify our numerical computations on this interval. Figure 4A shows the exact solutions as blue curve with the dot marker. The red curves in the same figure represent the numerical solutions at level $n = 9$ in this special case. The parameters are chosen to be the same in the exact and numerical solutions. In particular, we choose

$$R_0 = 1\ {\rm cm}, \quad C_0 = 2C_{\rm d,s}, \quad D_{\rm d} = 1.5 \times 10^{-6}\ {\rm cm^2 s^{-1}}, \quad \overline{k}_{\rm d} = 0.667.$$

Here, we choose $R_0 = 1$ cm to simplify the computation of $C_{\rm d}/C_{\rm d,s}$ using the explicit solution (34). We see that the numerical solutions match the exact solutions perfectly. Figure 4B shows that the numerical error decreases as the time evolves. Table III gives the magnitude of the error in the supremum norm for different time instances.

C. Comparison of Numerical and Approximate Solutions

It is always assumed in the mathematical models describing dispersed drug release that dissolution is much faster than diffusion. Moreover, in the limit of $\overline{k}_{\rm d} \to \infty$, the system of diffusion equations (5)–(6) (when again water penetration is neglected) reduces to the scalar diffusion equation with

TABLE III. The error of numerical computations in the supremum norm for different times.

t	1000 s	2000 s	3000 s	4000 s	5000 s
Error	4.3×10^{-5}	2.2×10^{-5}	1.5×10^{-5}	1.2×10^{-5}	8.0×10^{-6}

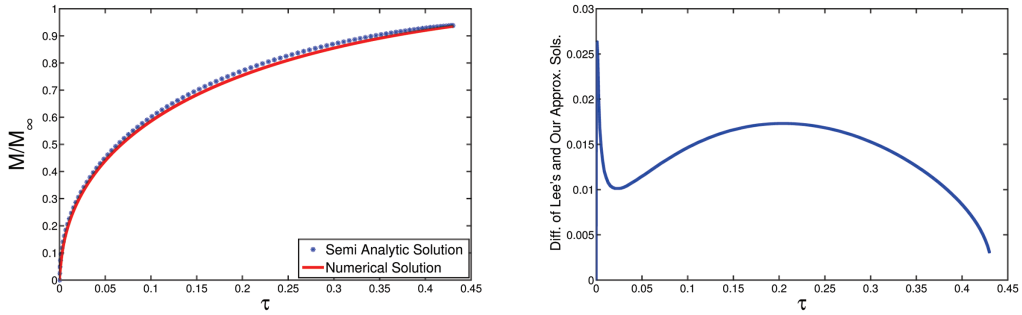

FIG. 5. Left: the numerical and approximate solutions for $M(\tau)/M_\infty$ in the system of diffusion equations (5)–(6) on $[t_0, t_*]$ in the case of no water and polymer erosion. Right: The distance between the two solutions. [Color figure can be viewed in the online issue, which is available at wileyonlinelibrary.com.]

an inner boundary,

$$\frac{\partial C_\mathrm{d}}{\partial t} = \frac{1}{r^2}\frac{\partial}{\partial r}\left(r^2 D_\mathrm{d}\frac{\partial C_\mathrm{d}}{\partial r}\right), \qquad \xi(t) < r < R(t), \tag{25}$$

The inner boundary $\xi(t)$ is determined by the boundary condition $C_\mathrm{d}(\xi(t), t) = C_{\mathrm{d,s}}$ and the mass balance equation,

$$(C_0 - C_{\mathrm{d,s}})\frac{d\xi(t)}{dt} = D_\mathrm{d}\frac{\partial C_\mathrm{d}}{\partial r}\bigg|_{r=\xi(t)}. \tag{26}$$

System (25)–(26) is valid for the time interval $[t_0, t_*]$, where t_0 is the time instance when $C_\mathrm{u}(R(t), t) = 0$ from Appendix A. Appendix B gives justification of system (25)–(26) in the limit $\overline{k}_\mathrm{d} \to \infty$.

An approximate analytical solution for system (25)–(26) in the case, when D_d is a constant and $R(t) = R_0$ is not moving, has been obtained by Lee [4]. Appendix C reviews details of derivation of this solution, which becomes an approximate solution for system (5)–(6).

The relative drug release is given by (45) and plotted as blue curve with cross marker in Fig. 5A for

$$R_0 = 0.1 \text{ cm}, \quad C_0 = 3C_{\mathrm{d,s}}, \quad D_\mathrm{d} = 1.0 \times 10^{-6} \text{ cm}^2\text{s}^{-1}.$$

Note that the relative release curve is reasonable for the drug release up to time $t_* = 4301$ s.

Let us now solve numerically system (5)–(6), where we remove the polymer swelling and erosion mechanisms and choose the dissolution rate much bigger than the diffusion coefficient. In particular, we choose $k_\mathrm{d} = 1.0 \times 10^{-1}\text{s}^{-1}$, which is reasonable in pharmaceutical research.

The numerical solution is plotted as red curve in Figure 5A. Those two curves are very close. Figure 5B shows the difference between these solutions. In particular, the error in the supremum norm is 0.0263.

This computation shows that the model (25)–(26) gives a good approximation for solutions of the system of diffusion equations (5)–(6) on the time interval $[t_0, t_*]$.

V. CONCLUSION

In this article, the dispersed drug release from hydrophilic polymer systems in spherical geometry is investigated by using a mathematical model incorporating diffusion, dissolution, swelling, and erosion mechanisms. We introduce a multilevel scheme to solve the governing diffusion equations and achieve a better approximation than the finite element method with lower computational costs. At the same level of accuracy, the multilevel scheme is much faster than the finite element method. The bigger the time step size is or the larger the linear system is, the more advantages our numerical multilevel scheme has over the finite element method. We also confirm that numerical solutions of the full model agree well with the exact and approximate solutions of the reduced models derived earlier.

APPENDIX A: EXACT SOLUTION FOR FIXED BOUNDARY ON $[0, t_0]$

We derive here an exact solution for the diffusion equation for dissolved drug,

$$\frac{\partial C_{\mathrm{d}}}{\partial t} = \frac{D_{\mathrm{d}}}{r^2}\frac{\partial}{\partial r}\left(r^2\frac{\partial C_{\mathrm{d}}}{\partial r}\right) + k_{\mathrm{d}}(C_{\mathrm{d,s}} - C_{\mathrm{d}}), \tag{27}$$

coupled together with the equation for dispersed drug,

$$\frac{\partial C_{\mathrm{u}}}{\partial t} = -k_{\mathrm{d}}(C_{\mathrm{d,s}} - C_{\mathrm{d}}). \tag{28}$$

We use the initial data,

$$t = 0, \;\; 0 \le r \le R_0 : \quad C_{\mathrm{d}} = C_{\mathrm{d,s}}, \quad C_{\mathrm{u}} = C_0 - C_{\mathrm{d,s}} > 0, \tag{29}$$

and the boundary conditions

$$t > 0, \;\; r = R_0 : \quad C_{\mathrm{d}} = 0. \tag{30}$$

This model corresponds to system (5)–(6) without considering polymer swelling and erosion under the assumption $C_{\mathrm{u}} > 0$. This assumption is only valid for an initial time interval $[0, t_0]$. We have also simplified the model by considering no water penetration and the fixed boundary of a polymer (no erosion). To justify the assumption $C_{\mathrm{u}} > 0$, we note that C_{u} drops fastest at $r = R_0$ and reaches zero at t_0 because $C_{\mathrm{d}} = 0$ at the surface and $C_{\mathrm{d}} > 0$ inside $(0, R_0)$. Integrate both sides of Eq. (28) from 0 to t_0 at R_0 and use the fact that $C_{\mathrm{u}}(R_0, t_0) = 0$, $C_{\mathrm{d}}(R_0, t) = 0$, and $C_{\mathrm{u}}(R_0, 0) = C_0 - C_{\mathrm{d,s}}$, we obtain

$$t_0 = \frac{C_0 - C_{\mathrm{d,s}}}{C_{\mathrm{d,s}} k_{\mathrm{d}}}.$$

To derive an exact solution for C_{d}, we use Eqs. (27), (29), and (30). Then, we solve for C_{u} by using Eqs. (28) and (29). Using the variable

$$u_{\mathrm{d}} = \frac{r C_{\mathrm{d}}}{C_{\mathrm{d,s}}} e^{k_{\mathrm{d}} t},$$

Eq. (27) becomes

$$\frac{\partial u_{\mathrm{d}}}{\partial t} - D_{\mathrm{d}} \frac{\partial u_{\mathrm{d}}}{\partial r^2} = k_{\mathrm{d}} r e^{k_{\mathrm{d}} t}, \tag{31}$$

subject to the initial data $u_{\mathrm{d}}(r,0) = r$ for $r \in [0, R_0]$ and the Dirichlet boundary conditions $u_{\mathrm{d}}(0,t) = u_{\mathrm{d}}(R_0,t) = 0$. We can use separation of variables to solve the inhomogeneous diffusion equation (31).

Expanding $u_{\mathrm{d}}(r,t)$ and $k_{\mathrm{d}} r e^{k_{\mathrm{d}} t}$ into

$$u_{\mathrm{d}}(x,t) = \sum_{n=1}^{\infty} u_n(t) \sin\left(\frac{n\pi r}{R_0}\right),$$

and

$$k_{\mathrm{d}} r e^{k_{\mathrm{d}} t} = \sum_{n=1}^{\infty} h_n(t) \sin\left(\frac{n\pi r}{R_0}\right), \quad h_n(t) = -\frac{2R_0 k_{\mathrm{d}} e^{k_{\mathrm{d}} t} \cos(n\pi)}{n\pi}.$$

and using the orthogonality of sine functions, we obtain an uncoupled system of differential equations,

$$\frac{du_n(t)}{dt} + D_{\mathrm{d}} \frac{n^2\pi^2}{R_0^2} u_n(t) = h_n(t) \tag{32}$$

complemented with the initial data

$$u_n(0) = -\frac{2R_0 \cos(n\pi)}{n\pi}. \tag{33}$$

Solving (32) and (33), we have

$$u_n(t) = -\frac{2R_0 \cos(n\pi)}{D_{\mathrm{d}} n^2\pi^2 + k_{\mathrm{d}} R_0^2} \left(\frac{R_0^2 k_{\mathrm{d}}}{n\pi} e^{k_{\mathrm{d}} t} + D_{\mathrm{d}} n\pi e^{-\frac{D_{\mathrm{d}} n^2\pi^2}{R_0^2} t} \right).$$

Therefore, the exact solution for (27) is

$$\frac{C_{\mathrm{d}}(r,t)}{C_{\mathrm{d,s}}} = \sum_{n=1}^{\infty} \frac{-2R_0 \cos(n\pi)}{D_{\mathrm{d}} n^2\pi^2 + k_{\mathrm{d}} R_0^2} \left(\frac{R_0^2 k_{\mathrm{d}}}{n\pi} + D_{\mathrm{d}} n\pi e^{-\frac{D_{\mathrm{d}} n^2\pi^2}{R_0^2} t - k_{\mathrm{d}} t} \right) \frac{1}{r} \sin\left(\frac{n\pi r}{R_0}\right). \tag{34}$$

Substitute (34) into Eq. (28), we obtain the exact solution for dispersed drug,

$$\frac{C_{\mathrm{u}}(r,t)}{C_{\mathrm{d,s}}} = \frac{C_0}{C_{\mathrm{d,s}}} - 1 - k_{\mathrm{d}} t + k_{\mathrm{d}} \sum_{n=1}^{\infty} \frac{E_n(t)}{r} \sin\left(\frac{n\pi r}{R_0}\right), \tag{35}$$

where

$$E_n(t) = \frac{-2R_0 \cos(n\pi)}{D_{\mathrm{d}} n^2\pi^2 + k_{\mathrm{d}} R_0^2} \left(\frac{D_{\mathrm{d}} n\pi R_0^2}{D_{\mathrm{d}} n^2\pi^2 + k_{\mathrm{d}} R_0^2} + \frac{R_0^2 k_{\mathrm{d}}}{n\pi} t - \frac{D_{\mathrm{d}} n\pi R_0^2}{D_{\mathrm{d}} n^2\pi^2 + k_{\mathrm{d}} R_0^2} e^{-\frac{D_{\mathrm{d}} n^2\pi^2}{R_0^2} t - k_{\mathrm{d}} t} \right).$$

These expressions are compared with numerical numerical solutions in Section IVC.

APPENDIX B: DERIVATION OF THE REDUCED MODEL ON $[t_0, t_*]$

We rewrite the system of diffusion equations (5)–(6) in the two domains $[0, \xi(t)]$ and $[\xi(t), R_0]$ separated by the boundary $r = \xi(t)$, where $C_{\rm u}(\xi(t), t) = 0$. This separation is valid for $t \in [t_0, t_*]$, where t_0 is defined in Appendix A as the first time instance when $C_{\rm u}(R_0, t) = 0$ and t_* is the time instance when $\xi(t) = 0$ (or $t_* = \infty$ if this does not happen in a finite time). In the first domain $r \in (0, \xi(t))$ for $t \in (0, t_*)$, we have

$$\frac{\partial C_{\rm d}}{\partial t} = \frac{1}{r^2}\frac{\partial}{\partial r}\left(r^2 D_{\rm d}\frac{\partial C_{\rm d}}{\partial r}\right) + k_{\rm d}(C_{\rm d,s} - C_{\rm d}), \tag{36}$$

$$\frac{\partial C_{\rm u}}{\partial t} = -k_{\rm d}(C_{\rm d,s} - C_{\rm d}), \tag{37}$$

subject to the boundary condition $\frac{\partial C_{\rm d}}{\partial r} = 0$ at $r = 0$ and the initial conditions $C_{\rm d} = C_{\rm d,s}$ and $C_{\rm u} = C_0 - C_{\rm d,s} > 0$ at $t = 0$. In the second domain $r \in (\xi(t), R(t))$ for $t \in (t_0, t_*)$ (when $\xi(t) < R_0$), we have

$$\frac{\partial C_{\rm d}}{\partial t} = \frac{1}{r^2}\frac{\partial}{\partial r}\left(r^2 D_{\rm d}\frac{\partial C_{\rm d}}{\partial r}\right), \tag{38}$$

subject to the boundary conditions $C_{\rm d} = 0$ at $r = R_0$. The inner boundary $\xi(t)$ is defined by the condition $C_{\rm u}(\xi(t), t) = 0$ and the continuity conditions for $C_{\rm d}$ and its derivative $\frac{\partial C_{\rm d}}{\partial r}$.

In the limit $\overline{k}_{\rm d} \to \infty$, we can neglect the small diffusion term in the first system (36)–(37) and obtain the constant solution of the initial-value problem for any $t \in (0, t_*)$ and $r \in [0, \eta(t)]$, where $\eta(t) < \xi(t)$ is fixed for any fixed t,

$$C_{\rm d}(r, t) = C_{\rm d,s}, \quad C_{\rm u}(r, t) = C_0 - C_{\rm d,s}. \tag{39}$$

We claim that for sufficiently small $\epsilon = 1/\overline{k}_{\rm d}$, there is constant $A > 0$ such that

$$\sup_{t\in[t_0,t_*]}\sup_{r\in[0,\eta(t)]}\left(\left|C_{\rm d} - C_{\rm d,s}\right| + \left|\frac{\partial C_{\rm d}}{\partial r}\right| + \left|C_{\rm u} - (C_0 - C_{\rm d,s})\right|\right) \le A\epsilon. \tag{40}$$

Neglecting the small remainder term and sending $\eta(t) \to \xi(t)$ for any $t \in (t_0, t_*)$, we can now close the second Eq. (38) as a boundary-value problem on $[\xi(t), R_0]$ subject to the boundary conditions $C_{\rm d} = C_{\rm d,s}$ at $r = \xi(t)$ and $C_{\rm d} = 0$ at $r = R_0$. This boundary-value problem is posed for $t \in (t_0, t_*)$ starting with the initial condition $C_{\rm d} = C_{\rm d,s}$ at $\xi(t) = R_0$ and $t = t_0$.

To determine the equation for the inner boundary $\xi(t)$, we represent the solution for $C_{\rm u}$ on $[0, R_0]$ by using the Heaviside step function H,

$$C_{\rm u}(r, t) = (C_0 - C_{\rm d,s})H(\xi(t) - r).$$

The diffusion equation (5) becomes now

$$r^2\frac{\partial C_{\rm d}}{\partial t} = \frac{\partial}{\partial r}\left(r^2 D_{\rm d}\frac{\partial C_{\rm d}}{\partial r}\right) - r^2\frac{\partial C_{\rm u}}{\partial t}.$$

Integrating over $r \in [\eta(t), \xi(t)]$, using bound (40), and sending $\eta(t) \to \xi(t)$ for any $t \in (t_0, t_*)$, we obtain

$$\int_{\eta(t)}^{\xi(t)} r^2 \frac{\partial C_\mathrm{d}}{\partial t} dr = r^2 D_\mathrm{d} \frac{\partial C_\mathrm{d}}{\partial r}\bigg|_{r=\eta(t)}^{r=\xi(t)} + (C_0 - C_{\mathrm{d,s}}) \frac{d\xi(t)}{dt} \int_{\eta(t)}^{\xi(t)} r^2 \frac{d}{dr} H(\xi(t) - r) dr,$$

and hence

$$0 = D_\mathrm{d} \xi(t)^2 \frac{\partial C_\mathrm{d}}{\partial r}\bigg|_{r=\xi(t)} - (C_0 - C_{\mathrm{d,s}}) \frac{d\xi(t)}{dt} \xi(t)^2,$$

which yields Eq. (26).

APPENDIX C: AN APPROXIMATE SOLUTION FOR THE REDUCED MODEL

There exists an exact solution of the reduced model (25)–(26) in the space of one dimension [1] when the boundary is fixed $R(t) = R_0$. In three dimensions, we can construct an approximate analytic solution by using a method developed by Lee [4].

Differentiating $C_\mathrm{d}(\xi(t), t) = C_{\mathrm{d,s}}$ with respect to t and using (25) and (26), we obtain

$$\left(\frac{\partial C_\mathrm{d}}{\partial r}\right)^2\bigg|_{r=\xi(t)} + (C_0 - C_{\mathrm{d,s}}) \frac{1}{r^2} \frac{\partial}{\partial r} \left(r^2 \frac{\partial C_\mathrm{d}}{\partial r}\right)\bigg|_{r=\xi(t)} = 0. \tag{41}$$

This additional condition is more convenient than (26).

By introducing variables

$$\theta = \frac{r}{R_0} \left(\frac{C_{\mathrm{d,s}} - C_\mathrm{d}}{C_{\mathrm{d,s}}}\right), \quad \tau = t \frac{D_\mathrm{d}}{R_0^2}, \quad \xi = \frac{R_0 - r}{R_0},$$

the model is transformed to the diffusion equation

$$\frac{\partial \theta}{\partial \tau} = \frac{\partial^2 \theta}{\partial \xi^2}, \quad 0 < \xi < \delta(\tau) := 1 - \frac{\xi(t)}{R_0}, \tag{42}$$

subject to the boundary conditions $\theta(\delta(\tau), \tau) = 0$ and $\theta(0, \tau) = 1$, and the mass balance equation

$$\frac{\partial \theta}{\partial \xi}\bigg|_{\xi=\delta(\tau)} = \left(1 - \frac{C_0}{C_{\mathrm{d,s}}}\right)(1 - \delta) \frac{d\delta}{d\tau}, \tag{43}$$

or equivalently,

$$\left(\frac{\partial \theta}{\partial \xi}\right)^2\bigg|_{\xi=\delta(\tau)} = \left(\frac{C_0}{C_{\mathrm{d,s}}} - 1\right)(1 - \delta) \frac{\partial^2 \theta}{\partial \xi^2}\bigg|_{\xi=\delta(\tau)}. \tag{44}$$

Double integration of (42) gives

$$\int_0^\delta dx \int_x^\delta \frac{\partial \theta}{\partial \tau} d\xi = \int_0^\delta dx \int_x^\delta \frac{\partial^2 \theta}{\partial \xi^2} d\xi.$$

Let us assume that there exists a self-similar solution $\theta(\xi,\tau) = \theta(\eta)$ of the diffusion equation (42) with $\eta = \xi/\delta$. Letting $y = x/\delta$ and integrating by parts, we obtain

$$\begin{aligned}\int_0^\delta dx \int_x^\delta \frac{\partial\theta}{\partial\tau} d\xi &= -\delta\frac{d\delta}{d\tau}\int_0^1 dy \int_y^1 \eta\frac{d\theta}{d\eta}d\eta \\ &= \delta\frac{d\delta}{d\tau}\left[\int_0^1 y\theta(y)dy + \int_0^1 dy\int_y^1 \theta d\eta\right] \\ &= 2\delta\frac{d\delta}{d\tau}\int_0^1 dy\int_y^1 \theta d\eta.\end{aligned}$$

On the other hand, using the boundary conditions and the mass balance equation (43), we obtain

$$\int_0^\delta dx\int_x^\delta \frac{\partial^2\theta}{\partial\xi^2}d\xi = \left(1-\frac{C}{C_{\rm d,s}}\right)(1-\delta)\delta\frac{d\delta}{d\tau} + 1.$$

Combining these two computations together, we have

$$\frac{d(g_1\delta^2 + g_2\delta^3)}{d\tau} = 1 \quad \Rightarrow \quad g_1\delta^2 + g_2\delta^3 = \tau,$$

where

$$g_1 = \int_0^1 dy\int_y^1 \theta d\eta + \frac{1}{2}\left(\frac{C_0}{C_{\rm d,s}} - 1\right) \quad \text{and} \quad g_2 = -\frac{1}{3}\left(\frac{C_0}{C_{\rm d,s}} - 1\right).$$

To approximate a solution, we need to properly choose θ as a function of η. Langford [23] showed that a quadratic polynomial gives a good accuracy,

$$\theta = a_1 + a_2\eta + a_3\eta^2,$$

if the coefficients are found from the boundary conditions and the mass balance equation (44),

$$\begin{aligned}&a_1 = 1,\\ &a_2 = -a_3 - 1,\\ &a_3 = 1 + \left(\frac{C_0}{C_{\rm d,s}} - 1\right)(1-\delta) - \sqrt{\left[1 + \left(\frac{C_0}{C_{\rm d,s}} - 1\right)(1-\delta)\right]^2 - 1}.\end{aligned}$$

Therefore, we have

$$\tau = \frac{1}{12}\left[6\left(\frac{C_0}{C_{\rm d,s}}\right) - 4 - a_3\right]\delta^2 - \frac{1}{3}\left(\frac{C_0}{C_{\rm d,s}} - 1\right)\delta^3.$$

The relative mass of the drug release in (11) is now approximated by the explicit expression,

$$\frac{M}{M_\infty} = [1-(1-\delta)^3]\left(1 - \frac{C_{\rm d,s}}{C_0}\right) + 3\delta\left(\frac{C_{\rm d,s}}{C_0}\right)\left[\left(a_1 + \frac{a_2}{2} + \frac{a_3}{3}\right) - \left(\frac{a_1}{2} + \frac{a_2}{3} + \frac{a_3}{4}\right)\delta\right]. \tag{45}$$

This expression is compared with numerical solutions in Section IVC.

The authors are grateful to Shirley Wu and Yousheng Zhou for introduction to the problem, inspiring discussions, and valuable references.

References

1. D. R. Paul and S. K. McSpadden, Diffusional release of a solute from a polymer matrix, J Membr Sci 1 (1976), 33–48.
2. N. Wu, L.-S. Wang, D. C.-W. Tan, S. M. Moochhala, and Y.-Y. Yang, Mathematical modeling and in vitro study of controlled drug release via a highly swellable and dissoluble polymer matrix: polyethylene oxide with high molecular weights, J Controlled Release 102 (2005), 569–581.
3. Y. Zhou and X. Y. Wu, Modeling and analysis of dispersed-drug release into a finite medium from sphere ensembles with boundary layer, J Controlled Release 90 (2003), 23–36.
4. P. I. Lee, Diffusional release of a solute from a polymeric matrix - approximate analytical solutions, J Membr Sci 7 (1980), 255–275.
5. X. Y. Wu and Y. Zhou, Studies of diffusional release of a dispersed solute from polymeric matrices by finite element method, J Pharm Sci 88 (1999), 1050–1057.
6. T. Higuchi, Rate of release of medicaments from ointment bases containing drugs in suspension, J Pharm Sci 50 (1961), 874–875.
7. T. Higuchi, Mechanism of sustained-action medication, J Pharm Sci 52 (1963), 1145–1149.
8. Y. Zhou and X. Y. Wu, Theoretical analysis of dispersed-drug release from planar matrices with a boundary layer in a finite volume, J Controlled Release 84 (2002), 1–13.
9. Y. Zhou, J. S. Chu, T. Zhou, and X. Y. Wu, Modeling of dispersed-drug release from two-dimensional matrix tablets, Biomaterials 26 (2005), 945–952.
10. A. Abbasi, M. Eslamian, and D. Rousseau, Modeling of caffeine Release from crosslinked water-swellable gelatin and gelatin-maltodextrin hydrogels, Drug Delivery 15 (2008), 455–463.
11. M. A. Christon and D. W. Roach, The numerical performance of wavelets for PDEs: the multi-scale finite element, Comput Mech 25 (2000), 230–244.
12. R.-Q. Jia and W. Zhao, Riesz bases of wavelets and applications to numerical solutions of elliptic equations, Math Comput 80 (2011), 1525–1556.
13. R. Stevenson, A robust hierarchical basis preconditioner on general meshes, Numer Math 78 (1997), 269–303.
14. H. Yserentant, The convergence of multi-level methods for solving > finite-element equations in the presence of singularities, Math Comput 47 (1986), 399–409.
15. D. S. Cohen, A. B. White, and T. P. Witelski, Shock formation in a multidimensional viscoelastic diffusive system, SIAM J Appl Math 55 (1995), 348–368.
16. D. A. Edwards, Constant front speed in weakly non-Fickian diffusive systems, SIAM J Appl Math 55 (1995), 1039–1058.
17. B. Rivière and S. Shaw, Discontinuous finite element approximation of nonlinear non-Fickian diffusion in viscoelastic polymers, SIAM J Numer Anal 44 (2006), 2650–2670.
18. K. Eriksson and V. Thomee, Galerkin methods for singular boundary value problems in one space dimension, Math Comput 43 (1984), 345–367.
19. P. Murray and G. F. Carey, Finite element analysis of diffusion with reaction at a moving boundary, J Comput Phys 74 (1988), 440–455.
20. H. G. Landau, Heat conduction in a melting solid, Q Appl Math 8 (1950), 81–94.
21. S.-T. Liu, Modified hierarchy basis for solving singular boundary value problems, J Math Anal Appl 325 (2007), 1240–1256.
22. D. Braess and W. Hackbusch, A new convergence proof for the multigrid method including the V-cycle, SIAM J Numer Math 9 (1966), 236–249.
23. D. Langford, The heat balance integral method, Intg J Heat Mass Transfer 16 (1973), 2424–2428.